Optimizing Operation Rules of Cascade Reservoirs for Adapting Climate Change

Shaokun He [1,2,3] · Shenglian Guo [1] · Guang Yang [1] · Kebing Chen [1] · Dedi Liu [1] · Yanlai Zhou [1]

Abstract

Climate change leads to great impact on hydrological cycle and consequently affects water resources management. Historical strategies are no longer applicable under a changing environment. Therefore, adaptive management, especially adaptive operation rules for reservoirs, has been developed to mitigate the potential adverse impacts of climate change. However, previous studies generally provide a similar framework for adaptation strategies of individual reservoir without consideration of cascade reservoirs in the future scenario. This study derives adapting operation rules for cascade reservoir system based on future projections (2021–2100) of two global climate change models (GCMs). By using Pareto archived dynamically dimensioned search (PA-DDS) algorithm with maximization of water supply and power generation, the performance of the adaptive operation rule curves is compared with the designed operation rule. The results demonstrate that Pareto solutions of the PA-DDS algorithm provide a wider, more optimal range of annual power generation and water supply, and the projection pursuit method can select the best. The adaptive operation rules focusing on power generation can significantly increase the cascade reservoir annual power generation (by 3.7% in GCM-BCC or 4.8% in GCM-BNU), which shows that the proposed method can adapt future climate change.

✉ Shenglian Guo
slguo@whu.edu.cn

Shaokun He
he_shaokun@whu.edu.cn

[1] State Key Laboratory of Water Resources and Hydropower Engineering Science, Wuhan University, Wuhan 430072, China

[2] Delft University Technology, Water Resources Section, 2601 DA Delft, the Netherlands

[3] IHE Delft Inst Water Educ, Hydroinformat Grp, Delft, the Netherlands

1 Introduction

Climate change, rapid socio-economic development and further growth of the human population are regarded as three major factors for increasing water-related issues. According to the Fifth Assessment Report of the Intergovernmental Panel on Climate Change (IPCC 2014), high greenhouse gas concentrations have led to increase in global average precipitation and temperature over land, particularly over high-latitude regions of the Northern hemisphere. Since the climate system is interactive with hydrological cycle, changes in precipitation and temperature would lead to impacts on river flows (Zhang et al. 2017), which may cause further stress on water resources management by altering the quality and quantity of water availability. Therefore, it is of great importance to adjust current water management strategy in the context of changing climate (Turner et al. 2017; Wu et al. 2017; Yang et al. 2016).

Reservoirs, as one of the most efficient infrastructure constructions in water resources management (Li et al. 2019; Xu et al. 2019), can be properly operated to mitigate the potential adverse impacts of climate change. It is particularly appropriate for many locations where water resources are limited and inter-annual climatic variability is high (Villarin 2019; Villarin and Rodriguez-Galiano 2019). Strong reliance on reservoirs may lead to major pressure from future changes, which requires a balance between climate change and its effects on water availability as well as the development of water demand (Majone et al. 2016; Tornes et al. 2014). A large number of researches have been focused on the integration of climate change and reservoir operation. Eum and Simonovic (2010) proposed an integrated water resources management system for a Korean river basin to derive the optimal rule curve for multipurpose reservoirs under three different climatic conditions. Georgakakos et al. (2012) used a decision model to assess the value of adaptive reservoir management versus traditional operation practices for Northern California under four future scenarios. Yang et al. (2016) compared the dynamic programming method and the non-dominated sorting genetic algorithm-II for deriving multipurpose operation rules to adapt to climate change and to alleviate the conflicts between future hydropower generation and water supply of China's Danjiangkou reservoir. All above literatures demonstrate that adaptive operation on reservoirs is useful to support water resources development and management under future climate change.

However, these research efforts generally provide a broadly similar framework for adaptation strategies of individual reservoir, which cannot meet practical requirement with more reservoirs being put into use (Yu et al. 2014). Although cascade reservoir reoperation is proven to deal with water supply and demand patterns well (He et al. 2019; Vonk et al. 2014), only a limited number of studies have been conducted to investigate the climate adaptability of such complex cascade reservoir over the past decades. Wondimagegnehu and Tadele (2015) dealt with evaluation of climate change on operation of the Blue Nile Basin cascade reservoir and used HEC-ReSim model to project the average annual power generation of each reservoir with comparison of the base period. Feng et al. (2018) evaluated the impacts of future climate changes on long-term hydropower generation in the Jinsha river and adopted a gravitational search algorithm to realize the generation maximization of the cascade hydropower stations. It further reveals that a derivation of joint operation rules for adaptation to climate change would be necessary in water resources planning and management (Lopez-Moreno et al. 2014).

The aim of the paper is to explore the impact of future climate change on cascade reservoir operation and to analyze the adaptive operation rules derived by the Pareto archived

dynamically dimensioned search (PA-DDS) algorithm (Asadzadeh and Tolson 2012). With a case study of Hanjiang River basin, one of the important strategic areas in China for the South-to-North Water Diversion Project, the adaptive operating rules are designed to alleviate the conflicts between future power generation and water supply while considering the climate change applied to future projections (2021–2100) of two Global Climate Change Models (GCMs). The rest of the paper is organized as follows: Section 2 describes the reservoir characteristics and data collection; Section 3 illustrates the multi-objective reservoir operation model and the optimization procedure for adapting climate change; Section 4 analyzes the performance of the adaptive rules; Section 5 ends with the conclusions.

2 Study Area and Data Collection

2.1 Hanjiang River Basin

The Hanjiang River basin (in Fig. 1) is located between 107 and 115°E longitude and 30–35°N latitude. The river has a main stream length of 1577 km with a drainage area of 159,000 km². It emerges from the southern of Qinling Mountain, flows from northwest to southeast and finally merges into the Yangtze River. This mountainous region lies in the humid zone with a subtropical monsoonal climate. The mean annual temperature ranges between 14 and 16 °C. Annual precipitation varies between 700 mm and 1100 mm with almost 70–80% of the total amount occurring in flood seasons (from May to October), during which the freak rainstorms in early summer and persistent rains in autumn often cause great floods.

The Ankang reservoir and Danjiangkou reservoirs are situated at the upper and middle reach of the Hanjiang River basin, respectively. The Ankang reservoir serves mainly for
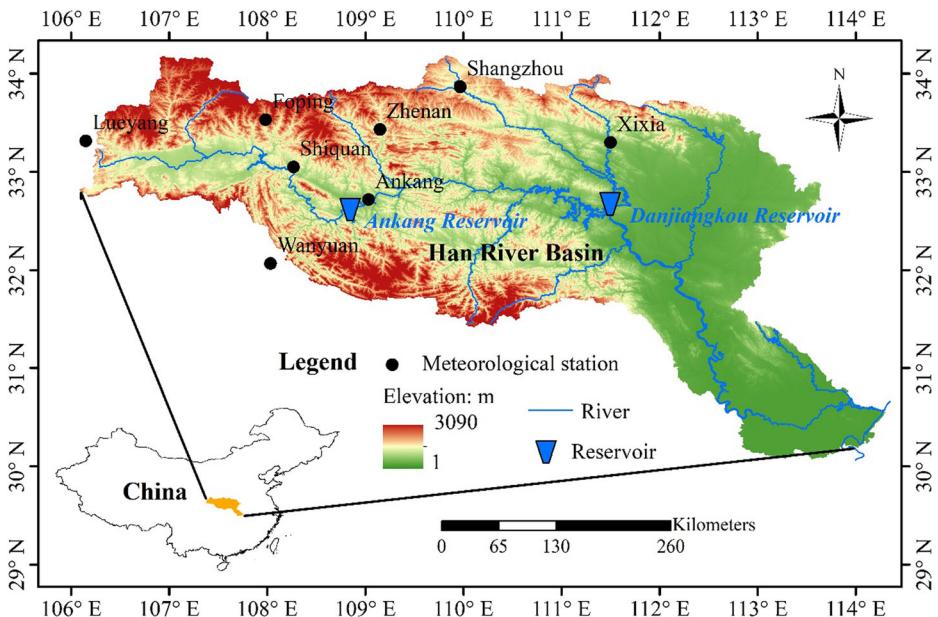

Fig. 1 Location of the Hanjiang River basin and two reservoirs

hydropower generation. The Danjiangkou reservoir is the only reservoir in Hangjiang basin involved in the Middle Route of the South-to-North Water Transfer Project in China for water supply. Its main functions include flood control, water supply, hydropower generation and irrigation. The characteristic parameter values of the Ankang and Danjiangkou reservoirs are given in Table 1 (Yang et al. 2017).

2.2 Reservoir Operation Rules

For the Ankang reservoir with its main function of hydropower generation, one form of reservoir operation rules (in Eq. (1)) proposed by Yeh (1985) is employed here for simplification since it was widely used in many operation rule researches (Celeste and Billib 2009; Yang et al. 2017): the water release of the Ankang reservoir ($Q_{out,\ t}$) is determined by the reservoir storage at the beginning of the current time period (V_t) and the inflow during the period for each 10-day period ($Q_{in,\ t}$):

$$Q_{out,t} = a_t \cdot \left(V_t + w \cdot Q_{in,t}\right) + b_t \ \ t = 1, ..., T \tag{1}$$

where a_t, b_t are volume and free coefficients in period t, respectively. w is a unit-converter coefficient.

The designed operation rule of Danjiangkou reservoir for water diversion formulated by Ministry of Water Resources (MWR 2016) is shown in Fig. 2. The reservoir water level should be maintained above 145 m during the entire operating period, but it must not exceed 160 m, 163.5 m and 170 m during summer flood season, autumn flood season and dry season, respectively. Water diversion decision is divided into five decision zones based on these water supply curves: reduce zone II, reduce zone I, normal zone, increase zone I and increase zone II. Each zone decides a fixed amount of water diversion according to the official regulation (MWR 2016). For example, if the water level at the beginning of November is lower than 147 m, water diversion reduction should be maintained below 20% of planned water supply, or if the water level is higher than 147 m but less than 155 m, water diversion reduction is fixed less than 15% of planned water supply. When water level falls into the normal zone, the flow for water diversion is the designed value. When water level rises into the increased zone I or increased zone II, the flow increment should not exceed 5% or 15% of planned water supply.

Table 1 Characteristic parameter values of the cascade reservoirs

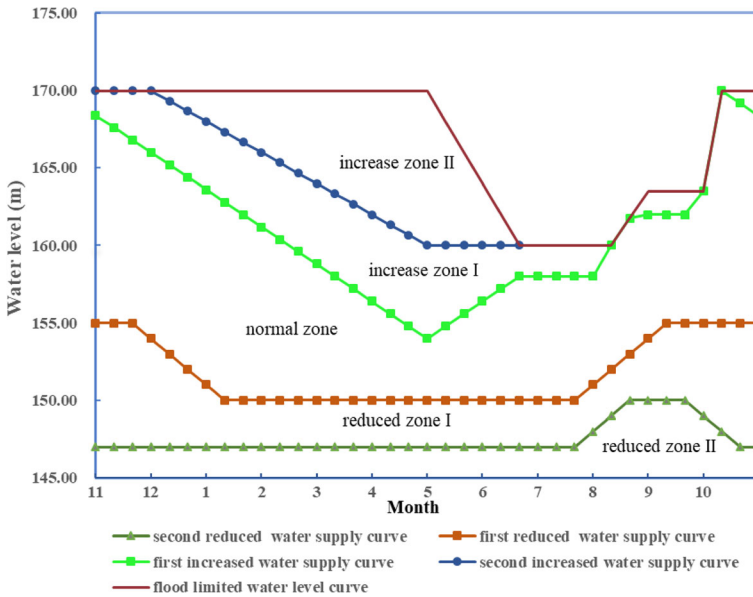| Reservoir	Ankang	Danjiangkou
Crest elevation (m)	338.0	176.6
Normal pool water level (m)	330.0	170.0
Flood limited water level in summer (m)	325.0	160.0
Flood limited water level in autumn (m)	325.0	163.5
Inactive water level (m)	305.0	150.0
Fluctuating water level (m)	300.0	145.0
Total storage capacity (billion m^3)	3.34	33.91
Flood control capacity in summer (billion m^3)	0.36	14.10
Flood control capacity in autumn (billion m^3)	0.36	11.10
Installed hydropower capability (MW)	800	900
Regulation ability	yearly	multi-year

Fig. 2 The designed operation rules for water diversion of Danjiangkou reservoir

2.3 Data

Observed daily precipitation and temperature data of 8 meteorological stations from 1971 to 2005 are collected from China Meteorological Data Sharing Service System (CMA 2018) and treated as the datasets of base period. These stations are evenly distributed over the Hanjiang River basin (Yang et al. 2016), their annual average precipitation, annual average maximum and minimum temperature data are shown in Table 2. The streamflow time series of 1980–2005 at Ankang station (the inflow of Ankang reservoir) and restored inflow of the Danjiangkou reservoir are provided by the Bureau of Hydrology of the Changjiang (Yangtze River) Water Resources Commission.

Climate change projections of future precipitation and temperature are generated from two GCMs under a greenhouse gas emission scenario. The two GCMs, i.e., the BCC-CSM1.1(m)

Table 2 Annual average precipitation and maximum, minimum temperature during 1971–2005 at 8 meteorological stations

Station	Station code	Latitude	Longitude	Temperature (°C)		Precipitation (mm)
				Minimum	Maximum	
Lueyang	57,106	33°19′	106°09′	9.5	19.1	793
Foping	57,134	33°32′	107°59′	7.7	18.2	899
Shangzhou	57,143	33°52′	109°58′	8.3	18.8	673
Zhenan	57,144	33°26′	109°09′	8.8	19.5	767
Xixia	57,156	33°18′	111°30′	10.8	20.8	845
Shiquan	57,232	33°03′	108°16′	10.6	20.3	883
Wanyuan	57,237	32°04′	108°02′	10.9	20.1	1245
Ankang	57,245	32°43′	109°02′	11.8	20.9	816

(GCM-BCC) and the BNU-ESM (GCM-BNU), are developed by Beijing Climate Center and Beijing Normal University, respectively. They have different horizontal resolutions (1.125° lat. ×1.125° long. For GCM-BCC and 2.8° lat. ×2.8° long. For GCM-BNU). We take both of them into our case study because both have good performance and wide applications in China (Shen et al. 2018; Wang et al. 2018). Although the Intergovernmental Panel on Climate Change (IPCC 2014) provides a new set of integrated scenarios to investigate some climate change issues, only Representative Concentration Pathway (RCP8.5) is accepted here as the worst case scenario, since the research basin is one of the most crucial strategic areas in China and decision-makers need to make the worst plan for the adequate preparation. The outputs of the GCM-BCC and GCM-BNU not only cover the historical period of 1971–2005 as a reference, but also cover 2021–2100 for the future period.

3 Methodology

The flowchart of multi-objective operation rules of cascade reservoirs for adapting climate change consists of the following three modules as shown in Fig. 3: (1) the outputs of precipitation and temperature are statistically downscaled into basin scale and used to project future flow discharge with the help of the Variable Infiltration Capacity (VIC) hydrological model; (2) the distribution of non-dominated solutions derived by the PA-DDS algorithm is
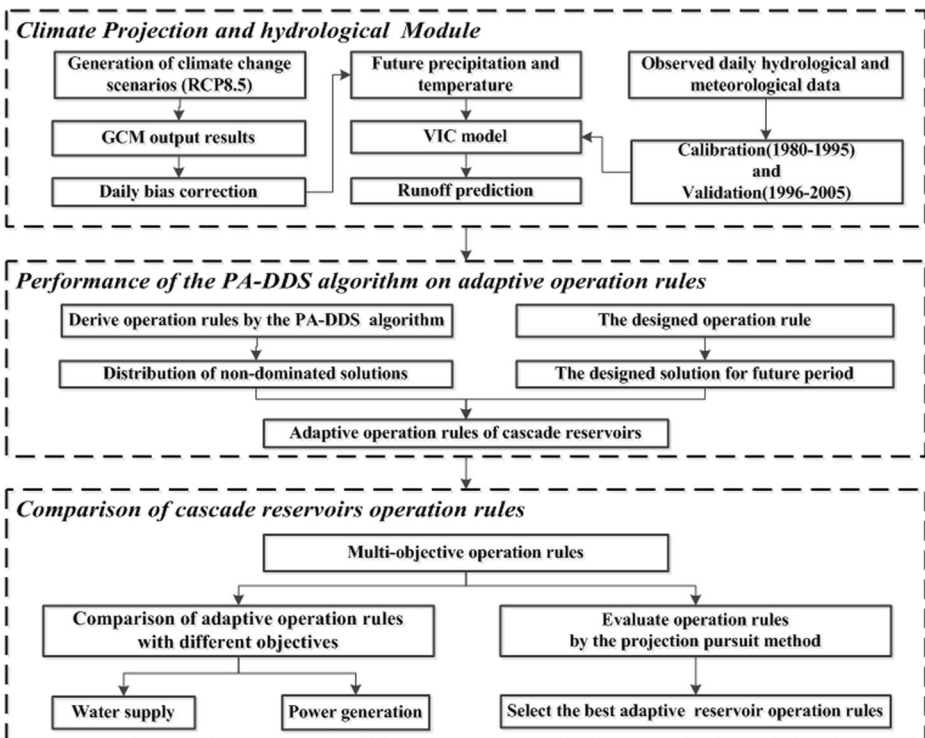

Fig. 3 Flowchart of multi-objective operation rules of cascade reservoirs for adapting climate change

analyzed with a reference of the designed solution; (3) the final module compares operation rules and determines the best one by projection pursuit method.

3.1 The Daily Bias Correction Method

Since the spatial resolution of GCM outputs is often too coarse and biased to be used directly by hydrological model for impact assessment, dynamical and statistical downscaling techniques have been proposed to bridge these gaps in the last decades (Wilby et al. 2002). Due to that both two GCMs in our study do not contain large-scale variables (atmospheric circulation factors) which serve as predictors for particular downscaling methods, such as artificial neural networks (Coulibaly et al. 2005), statistical downscaling model (Wilby et al. 2002), the daily bias correction method proposed by Chen et al. (2013) is applied in downscaling and bias correction for its ease of implementation and no need of large-scale variables.

The daily bias correction method is a hybrid method of combining the daily translation and the local intensity scaling method, which corrects not only the precipitation frequency and quantity, but also the frequency distributions of precipitation amounts and temperatures. The local intensity scaling method is firstly taken to correct the precipitation occurrence, to ensure that the frequency of the precipitation occurrence of corrected data series at the reference period equals that of the observed for a month. Then, instead of applying the same factor to scale the daily precipitation for a particular month, the daily translation method is adopted to modulate the changes as a function of percentile differences in the frequency distribution of precipitation (or temperature) between climate model and observation (Chen et al. 2013).

3.2 Runoff Simulation and Projection

Liang et al. (1994) introduced the VIC model, a macro-scale distributed hydrological model which has been widely used for flow forecasting and climate change impact studies. The VIC model has one kind of bare soil and different vegetation types in each grid cell. It contains both the saturation and infiltration excess runoff processes in a grid cell with a consideration of the sub grid-scale soil heterogeneity, and the frozen soil processes under the cold climate condition. The evaporation consists of three parts: evaporation from the canopy layer of each vegetation class, dry canopy and bare soil. The moisture transfer between soil layers obeys the Darcy law and the vertical soil is described by the one-dimensional Richard equation. The linear Saint-Venant method for channel flow and the routing model represented by the unit hydrograph method for overland flow, allow runoff to be predicted (Liang et al. 1994). The ability of the VIC model to simulate hydrological processes at a wide range of spatial scales has been well established through application to catchment ranging from small scales (Vonk et al. 2014) to continental and global scales (Endalamaw et al. 2017).

3.3 Objective Functions and Constraints

Two objective functions of maximizing water supply and power generation are involved in this study, which can be expressed as Eqs. (2) and (3):

$$Max \quad W = \sum_{i=1}^{M} \sum_{t=1}^{T} Q_{i,t}^{d} \cdot \Delta t \tag{2}$$

$$Max \quad E = \sum_{i=1}^{M} \sum_{t=1}^{T} N_{i,t} \cdot \Delta t, \quad N_{i,t} = K_i \cdot Q_{i,t}^{p} \cdot H_{i,t} \tag{3}$$

The constraints are listed as following:

(1) Water balance equation:

$$V_{i,t+1} = V_{i,t} + \left(Q_{i,t}^{in} - Q_{i,t}^{out} - Q_{i,t}^{d} \right) \cdot \Delta t - EP_{i,t} \tag{4}$$

(2) Connection of streamflow between reservoirs:

$$Q_{i,t}^{in} = Q_{i-1,t}^{out} + Q_{i,t}^{int} \tag{5}$$

(3) Reservoir water level limits:

$$Z_{i,t}^{min} \leq Z_{i,t} \leq Z_{i,t}^{max} \tag{6}$$

(4) Water requirement at downstream:

$$Q_{i,t}^{min} \leq Q_{i,t}^{out} \leq Q_{i,t}^{max}, Q_{i,t}^{out} = Q_{i,t}^{p} + Q_{i,t}^{s} \tag{7}$$

(5) Power generation limits:

$$P_{i,t}^{max} \leq N_{i,t} \leq P_{i,t}^{max} \tag{8}$$

(6) Boundary constraints:

$$Z_{i,t} = \begin{cases} Z_i^{begin} & t = 1 \\ Z_i^{end} & t = T \end{cases} \tag{9}$$

where

W (m³)	the sum of the water supply yield
E (kWh)	the total hydropower generation of cascade reservoirs
M	the number of reservoirs
T	the number of time periods
Δt (s)	the interval time during a single period
K_i	hydropower generation efficiency of the ith reservoir
$H_{i,t}$ (m)	average hydropower head of the ith reservoir at time t
$N_{i,t}$ (kW)	power output of the ith reservoir at time t
$V_{i,t}, V_{i,t+1}$ (m³)	the storage of the ith reservoir at time t and $t+1$, respectively.
$EP_{i,t}$ (m³)	sum of evaporation and leakage of the ith reservoir at time t.
$Q_{i,t}^{in}$ (m³/s)	inflow of the ith reservoir at time t
$Q_{i,t}^{out}$ (m³/s)	outflow discharge of the ith reservoir at time t
$Q_{i,t}^{d}$ (m³/s)	water supply flow of the ith reservoir at time t;

$Q_{1,t}^s$	is set 0 since the Ankang reservoir does not supply water for MSWTP
$Q_{i,t}^p$ (m³/s)	water release through turbine of the ith reservoir at time t
$Q_{i,t}^s$ (m³/s)	water release through spillway of the ith reservoir at time t
$Q_{i,t}^{int}$ (m³/s)	inflow of intervening basin between the i-1th and ith reservoir at time t
$Z_{i,t}$ (m)	water level of the ith reservoir at time t
$Z_{i,t}^{mini,t}$, $Z_{i,t}^{maxi,t}$ (m)	minimum and maximum water level of the ith reservoir at time t, respectively
$Q_{i,t}^{mini,t}$, $Q_{i,t}^{maxi,t}$ (m³/s)	minimum and maximum outflow discharge of the ith reservoir at time t, respectively
$P_{i,t}^{mini,t}$, $P_{i,t}^{maxi,t}$ (kW)	minimum and maximum power output of the ith reservoir at time t, respectively
Z_i^{begin}, Z_i^{end} (m)	beginning and terminal water level of the ith reservoir

3.4 Reservoir Operation Procedure

The designed operation rule curves of the Ankang reservoir are determined by the time-dependent variables a_t and b_t of Eq. (1). Since the time interval of long-term reservoir operation is 10 (or 11) days, there are 36 periods in a year and the total number of variables of the Ankang reservoir is 72 (36 × 2). These coefficients are determined by least-squares multiple regression (Karamouz and Houck 1982) to fit the linear relationship between the optimized $V_t + w \cdot Q_{in,t}$ and $Q_{out,t}$, after deterministic dynamic programming is used to obtain the optimal operation trajectories to maximize Eq.(3). For the downstream Danjiangkou reservoir, the first reduced water-supply curve of the operation rule is chosen for optimization due to its wide optimization scope for water resources potential. It can be described by 12 variables (5 and 7 variables in dry and flood seasons, respectively).

3.5 The PA-DDS Algorithm with Hyper-Volume Indicator

The PA-DDS algorithm, one of the popular and powerful meta-heuristic methods, is used here to solve the adaptive multi-objective operation. It inherits the Pareto-archived evolution strategy and uses only one parameter to archive all the non-dominated solutions. These widely distributed non-dominated solutions are also defined as Pareto front. An unary hyper-volume indicator can help rigorously define what is meant by "good spread of points" across a Pareto front, since it has good reputation on a guidance criterion for multi-objective solutions (Asadzadeh and Tolson 2013). Moreover, this indicator value can decide whether an evolutionary algorithm has better convergence, higher diversity and more even distribution of the Pareto front.

The detail procedures of the PA-DDS algorithm and the calculation of the hyper-volume indicator are further referred by Yang et al. (2017).

4 Results and Discussions

4.1 The Climate and Runoff Changes

The observed data series of 8 meteorological stations in the Hanjiang River basin during 1971–2005 are used to calibrate the daily bias correction method before downscaling of the future
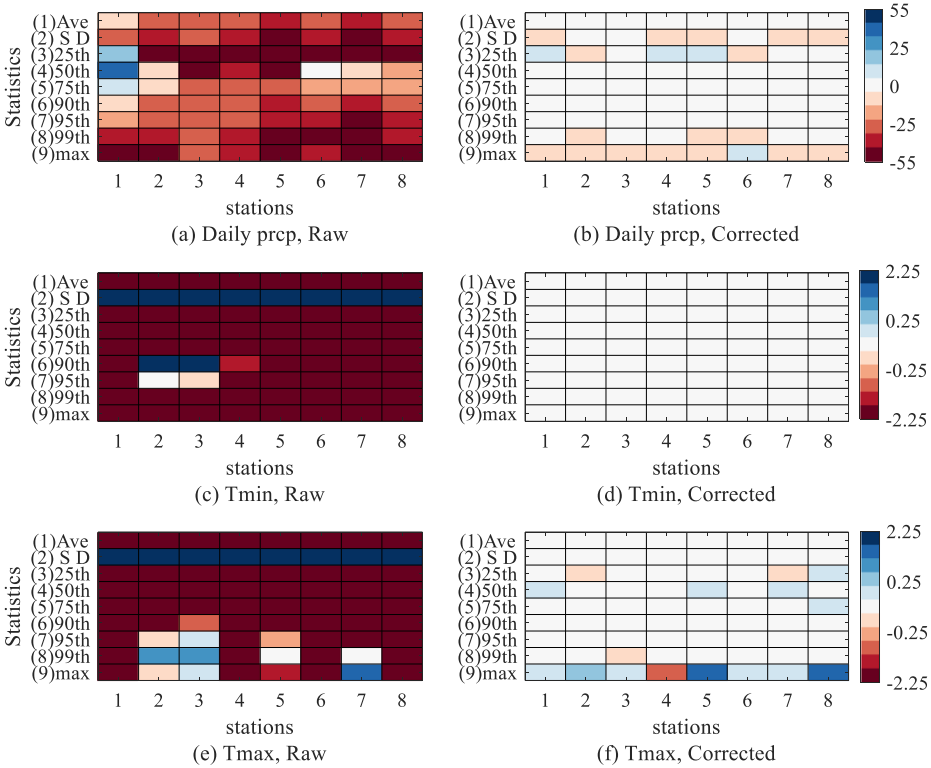
precipitation, maximum temperature (T_{max}) and minimum temperature (T_{min}). Nine statistics, i.e., mean, standard deviation, 25th, 50th, 75th, 90th, 95th and 99th percentiles and the maximum of precipitation (or temperature) series, are employed to evaluate the performance of the statistics downscaling method (Shen et al. 2018). The biases of raw and two corrected GCMs for precipitation and temperature at a daily scale in the reference period are presented in Fig. 4, where the lateral axis follows the 8 meteorological stations and the longitudinal axis shows the biases with respect to nine statistics. The bias is presented with respect to nine statistics, from y-axis number 1 to 9 representing average, standard deviation (SD), 25th, 50th, 75th, 90th, 95th, and 99th percentiles and maximum (max) value, respectively. The bias of precipitation and temperature are represented by the relative error and absolute error between GCM and observation, respectively. The raw GCMs are considerably with negative bias of simulated precipitation and temperature, while the evaluation indicators between the observation and GCMs are almost consistent after bias correction. All above results illustrate the reasonable performance of the daily bias correction method and it can be applied for generating future climate projection for hydrological impact studies.

After verifying the rationality of the downscaling method, the GCM-BCC and GCM-BNU outputs under RCP8.5 scenario with bias correction are employed to generate the daily
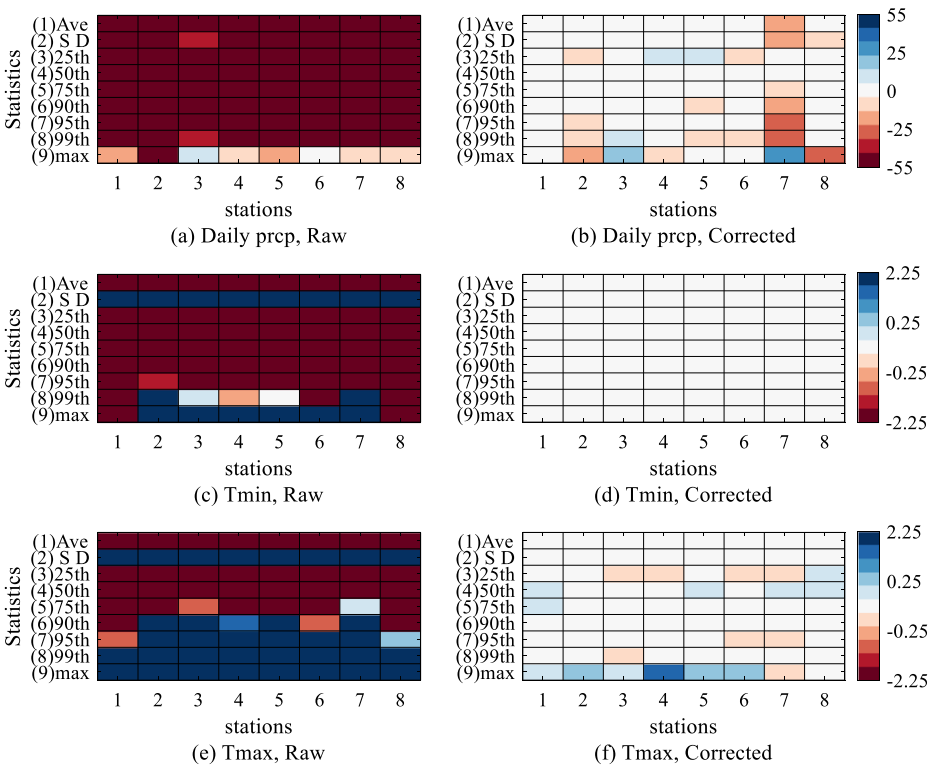
(I) GCM-BCC

Fig. 4 Bias of raw and corrected two GCM outputs, the x-axis means 8 meteorological stations, namely, Lueyang, Foping, Shangzhou, Zhenan, Xixia, Shiquan, Wanyuan, Ankang

(a) Daily prcp, Raw

(b) Daily prcp, Corrected

(c) Tmin, Raw

(d) Tmin, Corrected

(e) Tmax, Raw

(f) Tmax, Corrected

(II) GCM-BNU

Fig. 4 continued

precipitation and the maximum and minimum temperature during 2021~2100, which will furthermore impact the hydrological cycle and alter temporal and spatial variations of runoff (Wang et al. 2017). Table 3 shows a general increasing of annual mean precipitation of these representative meteorological stations in the future period except a significant decrease of precipitation of GCM-BCC at Wanyuan station. Meanwhile, a consistent absolute increase of temperature is predominant under two GCMs with change ranging between 0.1~1.9 °C and 0.1~2.5 °C, implying that the Hanjiang River basin is projected a warming trend under RCP8.5 scenario. The occurrence may be influenced by high greenhouse concentrations in this basin (Shen et al. 2018), following the conclusion that both precipitation and temperature are more likely to increase at a relatively higher rate with the most severe RCP 8.5 (Yin et al. 2018).

Meanwhile, daily hydrological and meteorological model data from 1980 to 1995 and 1996–2005 are used for calibration and validation, respectively. The Nash-Sutcliffe efficiency (NSE) and the relative error (RE) values of Ankang reservoir basin are 86.50% and 2.72%, 85.76% and 1.14% for calibration and validation periods, respectively. For the Danjiangkou reservoir basin, the NSE and RE values are 85.51% and 3.55%, 81.81% and 7.75% during calibration and validation periods, respectively. These results demonstrate that the VIC can simulate flow discharge well in Hanjiang River basin, since the NSEs of VIC are over 75% and its REs are within [−10%, 10%] in the calibration and validation periods (Gan et al. 2015).

Table 3 Projected future changes of annual average precipitation and temperature during 2021~2100 at 8 meteorological stations under two GCMs

Station	Variable	Historical period	GCM-BCC	GCM-BNU
Lueyang	Prep(mm)	793	820 (3.4%)	842 (6.2%)
	Temp(°C)	14.3	14.4 (0.1)	14.4 (0.1)
Foping	Prep(mm)	899	960 (6.8%)	965 (7.3%)
	Temp(°C)	13.0	14.6 (1.6)	15.0 (2.0)
Shangzhou	Prep(mm)	673	769 (14.3%)	756 (12.3%)
	Temp(°C)	13.6	15.5(1.9)	16.1 (2.5)
Zhenan	Prep(mm)	767	831 (8.3%)	840 (9.5%)
	Temp(°C)	14.2	15.5 (1.3)	16.2 (2.0)
Xixia	Prep(mm)	845	965 (14.2%)	924 (9.3%)
	Temp(°C)	15.8	17.4 (1.6)	17.8 (2.0)
Shiquan	Prep(mm)	883	936 (6.0%)	940 (6.5%)
	Temp(°C)	15.5	15.8 (0.3)	16.4 (0.9)
Wanyuan	Prep(mm)	1245	1006 (−19.2%)	1258 (1.0%)
	Temp(°C)	15.5	16.6 (1.1)	16.6 (1.1)
Ankang	Prep(mm)	816	857 (5.0%)	882 (8.1%)
	Temp(°C)	16.4	16.5 (0.1)	17.2 (0.8)

Values in parentheses represent the relative increment for precipitation and absolute increment for temperature of GCM prediction to historical observation

The streamflow projection at Ankang station and the intervening basin between Ankang and Danjiangkou reservoirs during 2021–2100 are used to assess climate change impact by the calibrated VIC model. The boxplot of monthly runoff results during base and future periods are compared and shown in Fig. 5. Only parts are reported here for the sake of saving space. It is observed that both the reservoir inflow and the intervening basin inflow in the future period under RCP8.5 scenario have a wider range compared with base period. Future runoff volume may remain consistent in the main flood season and increase in the dry season, which can reduce flood control pressure in flood seasons and somewhat alleviate the conflictions between power generation and water supply in dry seasons. In the meantime, annual runoff increase will make human activities more frequent in this area due to more economy benefits brought by abundant water resources; it will also boost agricultural development in the Han River basin via water transfer projects, where agricultural water demand has a largest partition (61.4%) (Tian et al. 2019). And reservoir operation is one of such effective measures to tap water potential (Yang et al. 2016).

4.2 Performance of the Adaptive Operation Rules

In the process of parameter setting of the PA-DDS algorithm, the maximum of the function evaluation is set as 15,000 to remain the unchanged value of the hyper-volume indicator, which sufficiently ensures that the algorithm can converge to a final steady state (Asadzadeh and Tolson 2013; Yang et al. 2017). As for another neighborhood perturbation size parameter r, a sensitivity analysis of it is carried out before optimizing the multi-objective operation rules of cascade reservoirs. A 12 independent hyper-volume indicator values of the non-dominated solutions with different parameter r suggest that the proper r value for the reservoir optimization should be 0.2, which is consistent with the default value recommended by Tolson and Shoemaker (2007).

(a) Ankang station

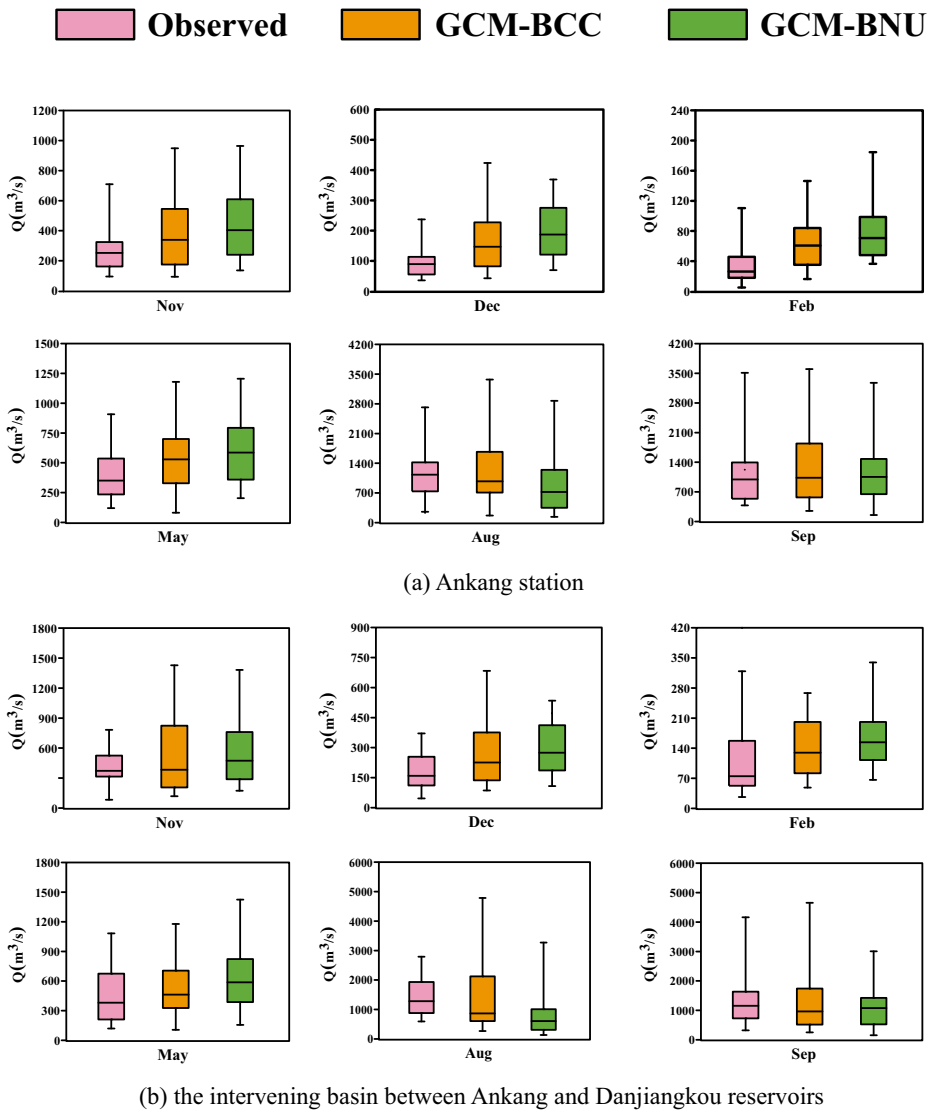(b) the intervening basin between Ankang and Danjiangkou reservoirs

Fig. 5 Boxplot of observed and projected monthly inflows at the Ankang station and intervening basin between Ankang and Danjiangkou reservoirs

In order to compare the designed operation rule with the adaptive operation rules, the results of all the rules are shown in Fig. 6. Evidently, the designed operation rule cannot be adapted to climate change for its relatively less water supply and power generation, while the adaptive perform well in this scenario. It is worthy noted that the dynamically dimensioned search strategy functions as the multi-objective search engine for the PA-DDS algorithm, which generally starts with global search in all dimensions of the decision space and reduces the number of variable dimensions with the search going on. It makes the PA-DDS algorithm excellent in both convergence speed and search ability when PA-DDS requires only one parameter (the neighborhood perturbation factor r) in extracting the multi-objective Danjiangkou reservoir operation rules.
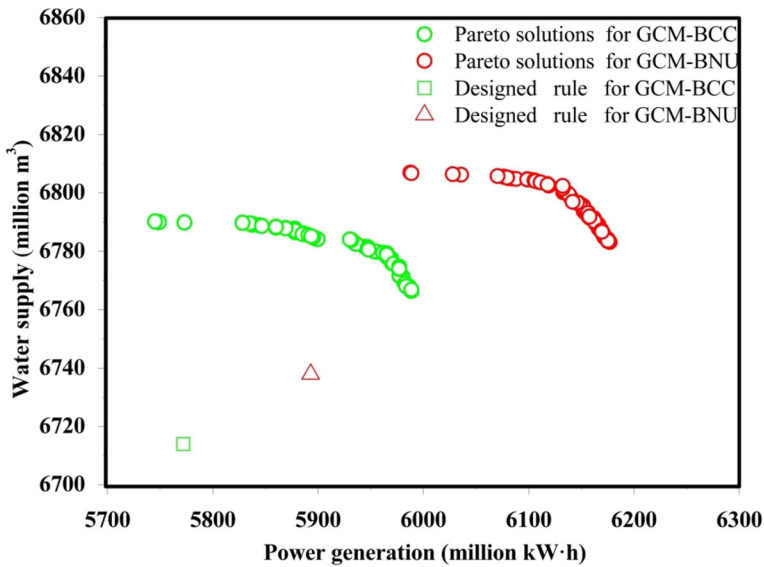
Fig. 6 Comparison of the designed operation rule with Pareto solutions of PA-DDS for GCMs

The optimization results of these rules for GCM-BCC and GCM-BNU have a wide range of power generation with a relatively concentrated distribution of water supply. Particularly, these solutions cover a wider range of power generation between 5738 and 5984 million kW.h in addition to proving a higher efficiency of water supply in GCM-BCC model. As for GCM-BNU model, it provides water supply yield fluctuating around 6800 million m³ and power generation range between 5987 and 6176 million kW.h.

4.3 Comparison of Operation Rules with Different Objectives

Since the rules aiming at maximizing one of the objectives can be helpful to strengthen the comprehension of multi-objective operations, the cascade reservoir operation results of two GCM models focusing on water supply and power generation are listed in Table 4.

In the objective of maximizing power generation for GCM-BCC, the adaptive operation rule can annually generate 5984 million kW.h hydropower (increase 3.7%) compared with the designed operation rule. Similarly, the adaptive operation rule for water supply can relatively improve water supply yield by 1.1% (from 6714 to 6790 million m³). For the GCM-BNU model, the adaptive operation rule for power generation can annually generate 6176 million kW.h, hydropower (increase 4.8%); the maximum average water supply is 1.0% higher than the reference value. In detail, the results reveal that the adaptive operation rules for power generation can rise average power generation by 6.1% in GCM-BCC and 4.8% in GCM-BNU than the designed operation rule during the dry season, respectively. The operation rule aiming at water supply is projected to annually increase water supply by 1.4% during dry season and 0.9% during flood season for GCM-BCC model. It also increases the average water supply by 1.3% and 0.7% during dry and flood seasons for GCM-BNU model, respectively. The increase rates of both objectives in the dry season are evidently higher than the flood season. The reason is that future inflow is projected to be more abundant in the dry season.

Table 4 Comparison of power generation and water supply calculated by designed and adaptive operation rules

GCM	Objective	Reservoir	Rules	Average power generation (million kW·h)			Average water supply (million m³)		
				Flood season	Dry season	Year	Flood season	Dry season	Year
BCC	Power generation	Ankang	design	1212	1118	2330	—	—	—
			adaptive	1222(0.8%)	1215(8.7%)	2437(4.6%)	—	—	—
		Danjiangkou	design	1757	1685	3442	3294	3420	6714
			adaptive	1789(1.8%)	1758(4.3%)	3547(3.1%)	3305(0.3%)	3461(1.2%)	6766(0.8%)
		Sum	design	2969	2803	5772	3294	3420	6714
			adaptive	3011(1.4%)	2973(6.1%)	5984(3.7%)	3305(0.3%)	3461(1.2%)	6766(0.8%)
	Water supply	Ankang	design	1212	1118	2330	—	—	—
			adaptive	1235(3.5%)	1136(1.6%)	2391(2.6%)	—	—	—
		Danjiangkou	design	1757	1685	3442	3294	3420	6714
			adaptive	1699(−3.3%)	1648(−2.2%)	3347(−2.7%)	3322(0.9%)	3468(1.4%)	6790(1.1%)
		Sum	design	2969	2803	5772	3294	3420	6714
			adaptive	2949(−0.7%)	2789(−0.5%)	5738(−0.6%)	3322(0.9%)	3468(1.4%)	6790(1.1%)
BNU	Power generation	Ankang	design	1223	1185	2408	—	—	—
			adaptive	1294(5.8%)	1239(4.6%)	2533(5.2%)	—	—	—
		Danjiangkou	design	1783	1702	3485	3302	3436	6738
			adaptive	1857(4.2%)	1786(4.9%)	3643(4.5%)	3318(0.5%)	3465(0.8%)	6783(0.7%)
		Sum	design	3006	2887	5893	3302	3436	6738
			adaptive	3151(4.8%)	3025(4.8%)	6176(4.8%)	3318(0.5%)	3465(0.8%)	6783(0.7%)
	Water supply	Ankang	design	1223	1185	2408	—	—	—
			adaptive	1271(3.9%)	1191(0.5%)	2462(2.2%)	—	—	—
		Danjiangkou	design	1783	1702	3485	3302	3436	6738
			adaptive	1812(1.6%)	1713(0.6%)	3525(1.1%)	3326(0.7%)	3481(1.3%)	6807(1.0%)
		Sum	Non-adaptive	3006	2887	5893	3302	3436	6738
			adaptive	3083(2.6%)	2904(0.6%)	5987(1.6%)	3326(0.7%)	3481(1.3%)	6807(1.0%)

Values in parentheses represent the relative change of the adaptive operation rules to the corresponding the designed operation rule

4.4 Selection of the Best Adaptive Operation Rule

The experiment indicates that the increase of water supply generally accompanies with the decrease of power generation. The best adaptive operation rule needs to be selected by considering the trade-offs between different objectives. The projection pursuit method (Friedman 1987) coupled with genetic algorithm, which can transform high dimensional data into one-dimensional data by unit projection vector, is used here to quantitatively describe the Pareto solutions and select the best one (Zhang et al. 2019).

Unit projection vectors obtained by genetic algorithm are 0.662 and 0.749, 0.638 and 0.770 for two different GCM models, respectively. It represents the relative importance of hydropower generation and water supply yield in our case study: the solutions with more water supply yield get higher one-dimensional projection values, meaning that the operation rules focusing on water supply are more suitable for cascade reservoirs in the Hanjiang River basin regardless of their poor performance in power generation. The higher weight of water supply corresponds to the vital role of the Danjiangkou reservoir for the Middle Route of the South-to-North Water Transfer Project in China.

The maximum comprehensive values are 1.252 for GCM-BCC and 1.306 for GCM-BNU. To show the characteristics of the operation rules, Fig. 7 gives some examples of the adaptive operation rules of the Ankang reservoir in Mid-Apr (dry season) and Mid-Aug (flood season). The Ankang reservoir operation rules are derived by the deterministic dynamic programming to fit future flow data under two GCMs. Different GCMs have the similar form of scheduling policy in the same period. Moreover, a "plane upper tail" phenomenon always occurs in the
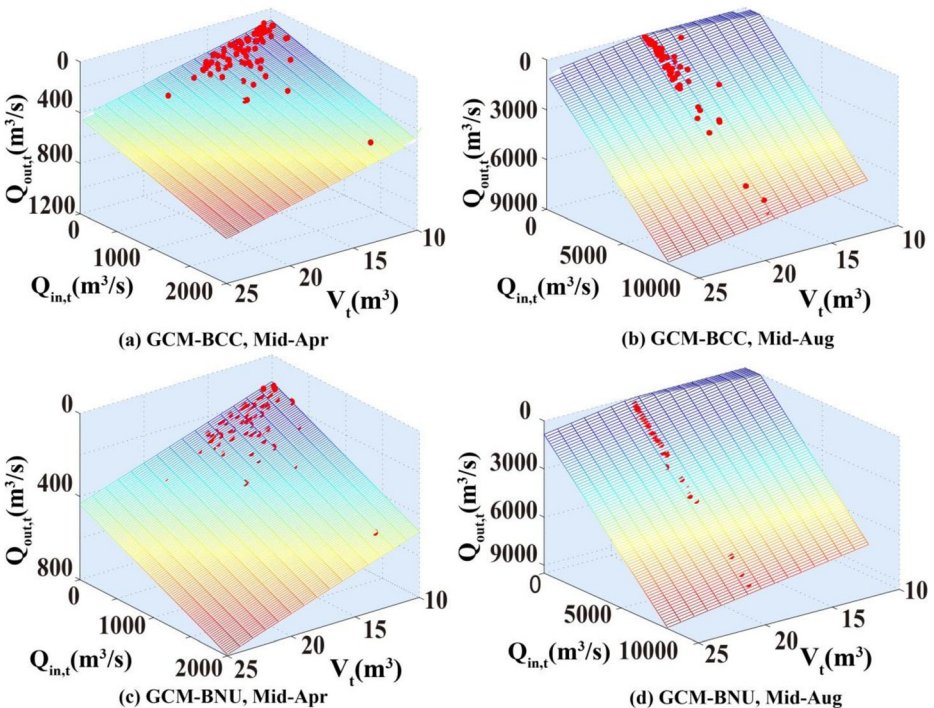

Fig. 7 Adaptive operation rules of the Ankang reservoir in Mid-Apr (dry season) and Mid-Aug (flood season)
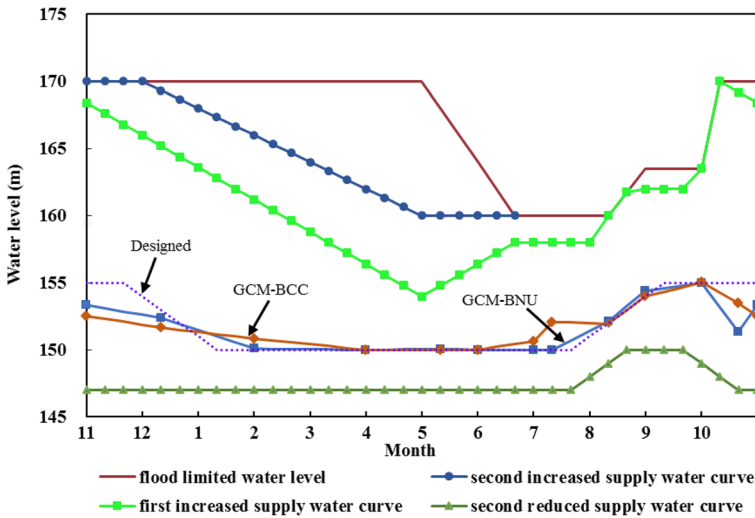
Fig. 8 Adaptive operation rule curves for water diversion of the Danjiangkou reservoir

optimal steady-state policy of the Ankang reservoir in the flood season. It is specifically shown in Fig. (7b) and (d) that the release discharge $Q_{out,\,t}$ of the Ankang reservoir remains unchanged and horizontal when function value of $V_t + w \cdot Q_{in,\,t}$ in Eq. (1) is small enough to be replaced by a plane scheduling rule. The reason is that reservoir release $Q_{out,\,t}$ should satisfy a constant downstream water requirement instead of an extreme situation with lower $V_t + w \cdot Q_{in,\,t}$ in flood season.

The adaptive water diversion curves of the Danjiangkou reservoir are plotted in Fig. 8, where the first reduced supply water curves of two GCMs have similar trendy that their positions move down in comparison with the designed curve. It shows that the area of water supply expands during the dry season and keeps almost same in the flood season. The reason is that projected future runoff increase in the dry season provides more possibilities for water supply scheduling rules by extending water supply area.

5 Conclusions

After downscaling GCM outputs in the Han River basin with the daily bias correction method, RCP 8.5 predicts a general increasing of annual mean precipitation and temperature in this area which will further results in future runoff increase. As more abundant future water resources can bring economy benefits and boost agriculture development, adaptive water policies should be further explored to tap water potential. Our study optimizes cascade reservoir operation rules based on future projections of two GCM models. In order to verify the performance of these operation rules, all the Pareto solutions are compared with the designed operation rule, and the projection pursuit method is used to select the best one. Some conclusions can be drawn as follows:

(1)   Under a high emission scenario, annual average temperature of 8 meteorological stations in the upper and middle Hanjiang River basin during 2021~2100 will increase 0.1~1.9 °C for GCM-BCC and 0.1~2.5 °C for GCM-BNU. The occurrence projects more runoff

during the dry season and stable runoff during the flood season, which also puts higher requirements on water resources management.

(2) The PA-DDS algorithm with hyper-volume selection is an effective method in searching Pareto front. All solutions achieve a widely distributed and better range of annual power generation with higher improvement of water supply. For the solution maximizing power generation, it can increase annual power generation by 3.7% in GCM-BCC model and 4.8% in GCM-BNU model, respectively, compared to the designed operation rule.

(3) For the optimal operation rule selected by projection pursuit theory, a "plane upper tail" phenomenon always accompanies with the optimal steady-state policy of Ankang reservoir during the flood season; The optimized first reduced supply water curve rules of the Danjiangkou reservoir have similar trendy under the two GCMs, both of which expand the area of water supply during the dry season.

References

Asadzadeh M, Tolson B (2012) Hybrid pareto archived dynamically dimensioned search for multi-objective combinatorial optimization: application to water distribution network design. J Hydroinf 14:192–205. https://doi.org/10.2166/hydro.2011.098

Asadzadeh M, Tolson B (2013) Pareto archived dynamically dimensioned search with hypervolume-based selection for multi-objective optimization. Eng Optim 45:1489–1509. https://doi.org/10.1080/0305215x.2012.748046

Celeste AB, Billib M (2009) Evaluation of stochastic reservoir operation optimization models. Adv Water Resour 32:1429–1443. https://doi.org/10.1016/j.advwatres.2009.06.008

Chen J, Brissette FP, Chaumont D, Braun M (2013) Performance and uncertainty evaluation of empirical downscaling methods in quantifying the climate change impacts on hydrology over two North American river basins. J Hydrol 479:200–214. https://doi.org/10.1016/j.jhydrol.2012.11.062

CMA (2018) China Meteorological Administration. http://data.cma.cn/

Coulibaly P, Dibike YB, Anctil F (2005) Downscaling precipitation and temperature with temporal neural networks. J Hydrometeorol 6:483–496. https://doi.org/10.1175/Jhm409.1

Endalamaw A, Bolton WR, Young-Robertson JM, Morton D, Hinzman L, Nijssen B (2017) Towards improved parameterization of a macroscale hydrologic model in a discontinuous permafrost boreal forest ecosystem. Hydrol Earth Syst Sc 21:4663–4680. https://doi.org/10.5194/hess-21-4663-2017

Eum HI, Simonovic SP (2010) Integrated reservoir management system for adaptation to climate change: the Nakdong river basin in Korea. Water Resour Manag 24:3397–3417. https://doi.org/10.1007/s11269-010-9612-1

Feng Y, Zhou JZ, Mo L, Yuan Z, Zhang PL, Wu J, Wang C, Wang YQ (2018) Long-term hydropower generation of cascade reservoirs under future climate changes in Jinsha river in southwest China. Water 10. https://doi.org/10.3390/w10020235

Friedman JH (1987) Exploratory projection pursuit J am stat Assoc 82:249-266. https://doi.org/10.2307/2289161

Gan YJ, Liang XZ, Duan QY, Choi HI, Dai YJ, Wu H (2015) Stepwise sensitivity analysis from qualitative to quantitative: application to the terrestrial hydrological modeling of a conjunctive surface-subsurface process (CSSP) land surface model. J Adv Model Earth Sy 7:648–669. https://doi.org/10.1002/2014ms000406

Georgakakos AP, Yao H, Kistenmacher M, Georgakakos KP, Graham NE, Cheng FY, Spencer C, Shamir E (2012) Value of adaptive water resources management in Northern California under climatic variability and change: Reservoir management. J Hydrol 412:34–46. https://doi.org/10.1016/j.jhydrol.2011.04.038

He SK, Guo SL, Chen KB, Deng LL, Liao Z, Xiong F, Yin JB (2019) Optimal impoundment operation for cascade reservoirs coupling parallel dynamic programming with importance sampling and successive approximation. Adv Water Resour 131. https://doi.org/10.1016/j.advwatres.2019.07.005

IPCC (2014) Climate change 2014: impacts adaptation and vulnerability and climate change 2014: mitigation of climate change. Contribution of working group II and working group III to the fifth assessment report of the IPCC

Karamouz M, Houck MH (1982) Annual and monthly reservoir operating rules generated by deterministic optimization. Water Resour Res 18:1337–1344. https://doi.org/10.1029/WR018i005p01337

Li JY, Zhong PA, Yang MZ, Zhu FL, Chen J, Xu B, Liu WF (2019) Dynamic and intelligent modeling methods for joint operation of a flood control system. J Water Resour Plan Manag 145. https://doi.org/10.1061/(Asce)Wr.1943-5452.0001110

Liang X, Lettenmaier DP, Wood EF, Burges SJ (1994) A simple hydrologically based model of land-surface water and energy fluxes for General-Circulation models. J Geophys Res-Atmos 99:14415–14428. https://doi.org/10.1029/94jd00483

Lopez-Moreno JI, Zabalza J, Vicente-Serrano SM, Revuelto J, Gilaberte M, Azorin-Molina C, Moran-Tejeda E, Garcia-Ruiz JM, Tague C (2014) Impact of climate and land use change on water availability and reservoir management: scenarios in the upper Aragon River. Spanish Pyrenees Sci Total Environ 493:1222–1231. https://doi.org/10.1016/j.scitotenv.2013.09.031

Majone B, Villa F, Deidda R, Bellin A (2016) Impact of climate change and water use policies on hydropower potential in the south-eastern Alpine region. Sci Total Environ 543:965–980. https://doi.org/10.1016/j.scitotenv.2015.05.009

MWR (2016) The designed operation rules of Danjiangkou reservoir for water diversion. Water Resources and Hydropower Press, Beijing (in Chinese)

Shen MX, Chen J, Zhuan MJ, Chen H, Xu CY, Xiong LH (2018) Estimating uncertainty and its temporal variation related to global climate models in quantifying climate change impacts on hydrology. J Hydrol 556: 10–24. https://doi.org/10.1016/j.jhydrol.2017.11.004

Tian J, Guo SL, Liu DD, Pan ZK, Hong XJ (2019) A fair approach for multi-objective water resources allocation. Water Resour Manag 33:3633–3653. https://doi.org/10.1007/s11269-019-02325-5

Tolson BA, Shoemaker CA (2007) Dynamically dimensioned search algorithm for computationally efficient watershed model calibration. Water Resour Res 43. https://doi.org/10.1029/2005wr004723

Tornes E, Perez MC, Duran C, Sabater S (2014) Reservoirs override seasonal variability of phytoplankton communities in a regulated Mediterranean river. Sci Total Environ 475:225–233. https://doi.org/10.1016/j.scitotenv.2013.04.086

Turner SWD, Ng JY, Galelli S (2017) Examining global electricity supply vulnerability to climate change using a high-fidelity hydropower dam model. Sci Total Environ 590:663–675. https://doi.org/10.1016/j.scitotenv.2017.03.022

Villarin MC (2019) Methodology based on fine spatial scale and preliminary clustering to improve multivariate linear regression analysis of domestic water consumption. Appl Geogr 103:22–39. https://doi.org/10.1016/j.apgeog.2018.12.005

Villarin MC, Rodriguez-Galiano VF (2019) Machine learning for modeling water demand. J Water Resour Plan Manag 145. https://doi.org/10.1061/(Asce)Wr.1943-5452.0001067

Vonk E, Xu YP, Booij MJ, Zhang X, DCM A (2014) Adapting multireservoir operation to shifting patterns of water supply and demand. Water Resour Manag 28:625–643. https://doi.org/10.1007/s11269-013-0499-5

Wang L, Guo SL, Hong XJ, Liu DD, Xiong LH (2017) Projected hydrologic regime changes in the Poyang Lake Basin due to climate change. Front Earth Sci-Prc 11:95–113. https://doi.org/10.1007/s11707-016-0580-5

Wang XJ, Zhang JY, Shahid S, Bi SH, Elmahdi A, Liao CH, Li YD (2018) Forecasting industrial water demand in Huaihe River Basin due to environmental changes. Mitig Adapt Strat Gl 23:469–483. https://doi.org/10.1007/s11027-017-9744-1

Wilby RL, Dawson CW, Barrow EM (2002) SDSM - a decision support tool for the assessment of regional climate change impacts. Environ Model Softw 17:147–159

Wondimagegnehu D, Tadele K (2015) Evaluation of climate change impact on Blue Nile Basin Cascade reservoir operation - case study of proposed reservoirs in the Main Blue Nile River basin. Ethiopia Proc IAHS 366: 133. https://doi.org/10.5194/piahs-366-133-2015

Wu XS, Wang ZL, Guo SL, Liao WL, Zeng ZY, Chen XH (2017) Scenario-based projections of future urban inundation within a coupled hydrodynamic model framework: a case study in Dongguan city. China J Hydrol 547:428–442. https://doi.org/10.1016/j.jhydrol.2017.02.020

Xu B, Zhu F, Zhong PA, Chen J, Liu W (2019) Identifying long-term effects of using hydropower to complement wind power uncertainty through stochastic programming. Appl Energy 253. https://doi.org/10.1016/j.apenergy.2019.113535

Yang G, Guo SL, Li LP, Hong XJ, Wang L (2016) Multi-objective operating rules for Danjiangkou reservoir under climate change. Water Resour Manag 30:1183–1202. https://doi.org/10.1007/s11269-015-1220-7

Yang G, Guo SL, Liu P, Li LP, Liu ZJ (2017) Multiobjective cascade reservoir operation rules and uncertainty analysis based on PA-DDS algorithm. J Water Resour Plan Manag 143. https://doi.org/10.1061/(Asce)Wr.1943-5452.0000773

Yeh WWG (1985) Reservoir management and operations models - a state-of-the-art review water Resour res 21: 1797-1818. https://doi.org/10.1029/WR021i012p01797

Yin JB, Gentine P, Zhou S, Sullivan SC, Wang R, Zhang Y, Guo SL (2018) Large increase in global storm runoff extremes driven by climate and anthropogenic changes. Nat Commun 9. https://doi.org/10.1038/s41467-018-06765-2

Yu PS, Yang TC, Kuo CM, Chou JC, Tseng HW (2014) Climate change impacts on reservoir inflows and subsequent hydroelectric power generation for cascaded hydropower plants. Hydrol Sci J 59:1196–1212. https://doi.org/10.1080/02626667.2014.912035

Zhang JW, Li ZJ, Wang X, Lei XH, Liu P, Feng MY, Khu ST, Wang H (2019) A novel method for deriving reservoir operating rules based on flood classification-aggregation-decomposition J Hydrol 568:722-734. https://doi.org/10.1016/j.jhydrol.2018.10.032

Zhang W, Liu P, Wang H, Chen J, Lei XH, Feng MY (2017) Reservoir adaptive operating rules based on both of historical streamflow and future projections. J Hydrol 553:691–707. https://doi.org/10.1016/j.jhydrol.2017.08.031